J. Fluid Mech. (2012), *vol.* 706, *pp.* 108–117. © Cambridge University Press 2012
doi:10.1017/jfm.2012.228

Effective slip boundary conditions for arbitrary one-dimensional surfaces

Evgeny S. Asmolov[1,2,3]† **and Olga I. Vinogradova**[1,4,5]

[1] A. N. Frumkin Institute of Physical Chemistry and Electrochemistry, Russian Academy of Sciences, 31 Leninsky Prospect, 119991 Moscow, Russia

[2] Central Aero-Hydrodynamic Institute, 140180 Zhukovsky, Moscow region, Russia

[3] Institute of Mechanics, M. V. Lomonosov Moscow State University, 119991 Moscow, Russia

[4] Department of Physics, M. V. Lomonosov Moscow State University, 119991 Moscow, Russia

[5] DWI, RWTH Aachen, Forckenbeckstr. 50, 52056 Aachen, Germany

(Received 3 March 2012; revised 21 April 2012; accepted 14 May 2012; first published online 7 June 2012)

In many applications it is advantageous to construct effective slip boundary conditions, which could fully characterize flow over patterned surfaces. Here we focus on laminar shear flows over smooth anisotropic surfaces with arbitrary scalar slip $b(y)$, varying in only one direction. We derive general expressions for eigenvalues of the effective slip-length tensor, and show that the transverse component is equal to half of the longitudinal one, with a two times larger local slip, $2b(y)$. A remarkable corollary of this relation is that the flow along any direction of the one-dimensional surface can be easily determined, once the longitudinal component of the effective slip tensor is found from the known spatially non-uniform scalar slip.

Key words: low-Reynolds-number flows, microfluidics, effective slip

1. Introduction

With recent advances in microfluidics (Stone, Stroock & Ajdari 2004), renewed interest has emerged in quantifying the effects on fluid motion of surface chemical heterogeneities with a different local scalar slip. In this situation it is advantageous to construct the effective slip boundary condition, which is applied at the imaginary smooth homogeneous, but generally anisotropic, surface and mimics the actual one along the true heterogeneous slip surface (Kamrin, Bazant & Stone 2010; Vinogradova & Belyaev 2011). Such an effective condition fully characterizes the flow at the real surface (on a scale larger than the pattern characteristic length) and can be used to solve complex hydrodynamic problems without tedious calculations.

For an anisotropic texture, the effective boundary condition generally depends on the direction of the flow and is a tensor, $\boldsymbol{b}_{eff} \equiv \{b_{ij}^{eff}\}$ represented by a symmetric, positive definite 2×2 matrix (Bazant & Vinogradova 2008)

$$\boldsymbol{b}_{eff} = \boldsymbol{S}_{\theta} \begin{pmatrix} b_{eff}^{\parallel} & 0 \\ 0 & b_{eff}^{\perp} \end{pmatrix} \boldsymbol{S}_{-\theta}, \tag{1.1}$$

† Email address for correspondence: AES50@yandex.ru

https://doi.org/10.1017/jfm.2012.228 Published online by Cambridge University Press

diagonalized by a rotation

$$\boldsymbol{S}_\theta = \begin{pmatrix} \cos\theta & \sin\theta \\ -\sin\theta & \cos\theta \end{pmatrix}. \tag{1.2}$$

Therefore, (1.1) allows us to calculate an effective slip in any direction given by an angle θ. In other words, the general problem reduces to computing the two eigenvalues, $b_{eff}^{\parallel}$ $(\theta = 0)$ and $b_{eff}^{\perp}$ $(\theta = \pi/2)$, which attain the maximal and minimal directional slip lengths, respectively. This tensorial slip approach, based on a consideration of a 'macroscale' fluid motion instead of solving hydrodynamic equations at the scale of the individual pattern, has been supported by statistical diffusion arguments (Bazant & Vinogradova 2008), and was recently justified for the case of Stokes flow over a broad class of periodic surfaces (Kamrin *et al.* 2010).

The concept of an effective tensorial slip has recently been proved by simulations (Priezjev 2011; Schmieschek *et al.* 2012), and has already been used to obtain simple solutions of several complex problems. It may be useful in many situations, such as drainage of thin films (Belyaev & Vinogradova 2010*b*; Asmolov, Belyaev & Vinogradova 2011), mixing in superhydrophobic channels (Vinogradova & Belyaev 2011), and electrokinetics of patterned surfaces (Bahga, Vinogradova & Bazant 2010; Belyaev & Vinogradova 2011). However, to the best of our knowledge all these analytical solutions were obtained for a flow on alternating slip and no-slip stripes, and the quantitative understanding of effective slippage past other types of anisotropic surfaces is still a challenge.

In this paper, we study the Stokes flow past flat surfaces, where the local (scalar) slip length b varies only in one direction. Our focus is on the limit of a thick (compared to texture period) channel or a single interface, so that effective slip is a characteristic of a heterogeneous interface solely and does not depend on the channel thickness. We derive a simple universal relationship between eigenvalues of the slip-length tensor. This allows one to avoid tedious calculations of flows in a transverse configuration, by reducing the problem to an analysis of longitudinal flows, which is much easier to evaluate. Our results open the possibility of solving a broad class of hydrodynamic problems for one-dimensional textured surfaces.

2. Theory

2.1. *General consideration*

We consider a creeping flow along a plane anisotropic wall, and a Cartesian coordinate system (x, y, z) (figure 1). The origin of coordinates is placed at the flat interface, characterized by a slip length $b(y)$, spatially varying in one direction, and the texture varies over a period L. Our analysis is based on the limit of a thick channel or a single interface, so that the velocity profile sufficiently far above the surface may be considered as a linear shear flow. Note that our results do not apply to a thin or an arbitrary channel situation, where the effective slip scales with the channel width (Feuillebois, Bazant & Vinogradova 2009; Schmieschek *et al.* 2012).

Dimensionless variables are defined by using L as a reference length scale, the shear rate sufficiently far above the surface, G, and the fluid kinematic viscosity, ν. We seek the solution for the velocity profile in the form

$$\boldsymbol{v} = \boldsymbol{U} + \boldsymbol{u}_1, \tag{2.1}$$

https://doi.org/10.1017/jfm.2012.228 Published online by Cambridge University Press

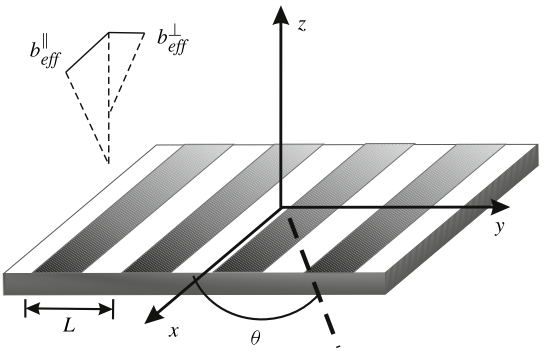


FIGURE 1. Schematic representation of periodic textures with scalar slip boundary conditions, varying in direction y. The patterns of slip boundary conditions are depicted as alternating stripes with piecewise-constant slip lengths, but our discussion is more general and applies to any one-dimensional distribution of a local slip (e.g. sinusoidal, trapezoidal, etc.).

where $\boldsymbol{U} = z\boldsymbol{e}_l$, $l = x, y$, is the undisturbed linear shear flow, and $\boldsymbol{e}_l$ are the unit vectors. The perturbation of the flow, $\boldsymbol{u}_1 = (u, v, w)$, which is caused by the presence of the texture and decays far from the surface at small Reynolds number $Re = GL^2/\nu$ satisfies dimensionless Stokes equations,

$$\nabla \cdot \boldsymbol{u}_1 = 0, \tag{2.2a}$$

$$\nabla p - \Delta \boldsymbol{u}_1 = \boldsymbol{0}, \tag{2.2b}$$

where p is pressure. The boundary conditions at the wall and at infinity are defined in the usual way

$$z = 0: \quad \boldsymbol{u}_{1\tau} - \beta\,(y)\,\frac{\partial \boldsymbol{u}_{1\tau}}{\partial z} = \beta\,(y)\,\boldsymbol{e}_l, \tag{2.3}$$

$$w = 0, \tag{2.4}$$

$$z \to \infty: \quad \frac{\partial \boldsymbol{u}_1}{\partial z} = \boldsymbol{0}, \tag{2.5}$$

where $\boldsymbol{u}_{1\tau} = (u, v, 0)$ is the velocity along the wall and $\beta = b/L$ is the normalized slip length.

A local slip length can be expanded in a Fourier series

$$\beta\,(y) = \sum_{n=-\infty}^{\infty} b^*\,(n) \exp\left(\mathrm{i}k_n y\right), \tag{2.6}$$

$$k_n = 2\pi n. \tag{2.7}$$

Similarly, the solution to (2.2) for $\boldsymbol{u}_1$ and p has the form

$$\boldsymbol{u}_1 = \sum_{n=-\infty}^{\infty} \boldsymbol{u}^*(n, z) \exp(\mathrm{i}k_n y), \quad p = \sum_{n=-\infty}^{\infty} p^*(n, z) \exp(\mathrm{i}k_n y), \tag{2.8}$$

and the Stokes equations can then be rewritten as

$$\nabla^* \cdot \boldsymbol{u}^* = 0, \tag{2.9}$$

$$\nabla^* p^* - \Delta^* \boldsymbol{u}^* = \boldsymbol{0}, \tag{2.10}$$

https://doi.org/10.1017/jfm.2012.228 Published online by Cambridge University Press

$$\boldsymbol{\nabla}^* = \left(0, \mathrm{i}k_n, \frac{\mathrm{d}}{\mathrm{d}z}\right), \quad \Delta^* = \frac{\mathrm{d}^2}{\mathrm{d}z^2} - k_n^2. \tag{2.11}$$

We have therefore reduced the problem to a system of ordinary differential equations (ODE), which can be now solved analytically. A similar strategy has been used before to address different hydrodynamic problems (Asmolov 2008; Davis & Lauga 2010; Kamrin *et al.* 2010).

The zero-mode solution represents a constant, $\boldsymbol{u}^*(0, z) = (c_x(0), c_y(0), 0)$. The eigenvalues of the effective slip-length tensor can be obtained as the components of $\boldsymbol{u}^*(0, z)$:

$$b_{eff}^{\parallel} = Lc_x(0), \quad b_{eff}^{\perp} = Lc_y(0). \tag{2.12}$$

Below we analyse in more detail two configurations of the shear flow, where the slip regions are distributed parallel ($\theta = 0$) and transverse ($\theta = \pi/2$) to the shear flow direction.

2.2. *Longitudinal configuration*

For longitudinal patterns, $\boldsymbol{U} = z\boldsymbol{e}_x$, so that the perturbation of the velocity has only one component, $\boldsymbol{u}_1 = (u, 0, 0)$, and the system (2.9)–(2.10) reduces to a single ODE:

$$\Delta^* u^* = 0. \tag{2.13}$$

Its solution that decays at infinity for non-zero modes has the form

$$u^* = c_x(n) \exp(-|k_n|z). \tag{2.14}$$

The boundary condition at the wall, (2.3), then determines constants $c_x(n)$. Indeed, from (2.8) and (2.14) we get

$$z = 0: \quad u = \sum_{n=-\infty}^{\infty} c_x(n) \exp(\mathrm{i}k_n y), \quad \frac{\partial u}{\partial z} = -\sum_{n=-\infty}^{\infty} |k_n| c_x(n) \exp(\mathrm{i}k_n y), \tag{2.15}$$

so that (2.3) takes the form

$$c_x(n) + \sum_{m=-\infty}^{\infty} |k_m| c_x(m) b^*(n-m) = b^*(n), \tag{2.16}$$

where $b^*(n)$ is the Fourier coefficient of the slip length. Thus we reduce the longitudinal problem to an infinite linear system for $c_x(n)$, which can be found by truncating the system and by using standard routines for linear systems.

2.3. *Transverse configuration*

For transverse patterns, $\boldsymbol{U} = z\boldsymbol{e}_y$ and $\boldsymbol{u}_1 = (0, v, w)$, the solution is usually constructed using the vorticity $\omega = \boldsymbol{\nabla} \times \boldsymbol{u}_1 = (0, 0, \omega_z)$, which significantly complicates the analysis compared to a longitudinal case (Cottin-Bizonne *et al.* 2004; Priezjev, Darhuber & Troian 2005; Belyaev & Vinogradova 2010*a*). However, simple analytical solutions can be obtained directly for the Fourier coefficients of velocities (Asmolov 2008; Kamrin *et al.* 2010). Indeed, (2.9)–(2.10) for transverse stripes can be written as

$$\mathrm{i}k_n v^* + \frac{\mathrm{d}w^*}{\mathrm{d}z} = 0, \tag{2.17a}$$

$$\mathrm{i}k_n p^* - \Delta^* v^* = 0, \tag{2.17b}$$

$$\frac{\mathrm{d}p^*}{\mathrm{d}z} - \Delta^* w^* = 0. \tag{2.17c}$$

https://doi.org/10.1017/jfm.2012.228 Published online by Cambridge University Press

By excluding p^* and v^*, one can transform them to a single ODE for the z-component:

$$\Delta^{*2} w^* = 0, \tag{2.18}$$

$$z = 0; \quad z \to +\infty : \quad w^* = 0. \tag{2.19}$$

A general solution of the fourth-order ODE (2.18) decaying at infinity can be written as

$$w^* = (c_z + d_z z)\exp(-|k_n|z). \tag{2.20}$$

Condition (2.19) then determines the coefficient, $c_z = 0$. The velocity Fourier coefficient in the y-direction can also be obtained from (2.17*a*):

$$v^* = c_y \exp(-|k_n|z)(1 - |k_n|z), \tag{2.21}$$

with $c_y = \mathrm{i}d_z/k_n$, so that

$$w^* = -\mathrm{i}k_n c_y z \exp(-|k_n|z). \tag{2.22}$$

Thus the solution for a given Fourier mode involves only one unknown constant $c_y(n)$, which can be found by applying boundary conditions (2.3). Using (2.8) and (2.21), we then get

$$z = 0 : \quad v = \sum_{n=-\infty}^{\infty} c_y(n)\exp(\mathrm{i}k_n y), \qquad \frac{\partial v}{\partial z} = -2\sum_{n=-\infty}^{\infty} |k_n| c_y(n)\exp(\mathrm{i}k_n y), \tag{2.23}$$

so that the slip boundary condition (2.3) can be rewritten as

$$c_y(n) + 2\sum_{m=-\infty}^{\infty} |k_m| c_y(m) b^*(n-m) = b^*(n). \tag{2.24}$$

The system (2.24) is very similar to that for the longitudinal patterns, (2.16), and differs only by the prefactor of 2. This means that the solution for $c_y(n)$ can be expressed in terms of coefficients $c_{x2}(n)$ for the longitudinal flow with two times the local slip, $b_2(y) = 2b(y)$. Since $b_2^*(n) = 2b^*(n)$, we obtain from (2.16)

$$c_{x2}(n) + 2\sum_{m=-\infty}^{\infty} |k_m| c_{x2}(m) b^*(n-m) = 2b^*(n). \tag{2.25}$$

The left-hand sides of the linear systems (2.24) and (2.25) are identical, but the right-hand sides differ by the factor of 2. In what follows,

$$c_y(n) = \frac{c_{x2}(n)}{2}. \tag{2.26}$$

Whence by using (2.12) we get

$$b_{eff}^{\perp}[b(y)/L] = \frac{b_{eff}^{\parallel}[2b(y)/L]}{2}. \tag{2.27}$$

Thus, the longitudinal and transverse effective slip lengths are affine, being related by a simple formula.

3. Discussion

In this section we compare (2.27) with the results obtained earlier for some particular periodic textures spatially varying in one direction y along the surface.

https://doi.org/10.1017/jfm.2012.228 Published online by Cambridge University Press

We also make use of (2.26) to prove a similarity of velocity profiles in eigendirections, again by giving some supporting examples from prior work. Finally, we show that our results are valid for arbitrary, not necessarily periodic, one-dimensional textures (varying on a characteristic scale L).

3.1. *Effective slip length*

During the last few decades several theoretical papers have been concerned with the flow past alternating (parallel or transverse) stripes characterized by piecewise-constant slip lengths, b^+ and b^-, with area fractions ϕ^+ and $\phi^- = 1 - \phi^+$, correspondingly. Without loss of generality we consider below that $0 \leqslant b^- \leqslant b^+ < \infty$. A large fraction of these papers deals with an ideal case of stripes with $b^+ \gg L$ (perfect slip) and $b^- = 0$ (no-slip). A formula describing the effective slip in the longitudinal direction for such a texture was proposed by Philip (1972):

$$b^{\parallel}_{ideal} = \frac{L}{\pi} \ln\left[\sec\left(\frac{\pi\phi^+}{2}\right)\right]. \tag{3.1}$$

Later Lauga & Stone (2003) derived an expression for the transverse configuration:

$$b^{\perp}_{ideal} = \frac{L}{2\pi} \ln\left[\sec\left(\frac{\pi\phi^+}{2}\right)\right], \tag{3.2}$$

which suggested that transverse and longitudinal components of the slip-length tensor are related as

$$b^{\perp}_{ideal} = \frac{b^{\parallel}_{ideal}}{2}. \tag{3.3}$$

This relationship is consistent with predictions of (2.27). Note that (3.3) should be valid not only for regular textures, such as shown in figure 1, but also for periodic textures including several stripes of differing widths, e.g. for hierarchical fractal surfaces (Cottin-Bizonne, Barentin & Bocquet 2012).

A few authors have discussed the situation of $b^- = 0$ and finite b^+. Numerical data obtained by Cottin-Bizonne *et al.* (2004) seem to satisfy (2.27), and their $b^{\parallel}_{eff}$, $b^{\perp}_{eff}$ asymptotically tend to the limiting values, $b^{\parallel}_{ideal}$ and $b^{\perp}_{ideal}$, when b^+/L becomes large. Belyaev & Vinogradova (2010*a*) derived analytical expressions for this case:

$$b^{\parallel}_{eff} \simeq \frac{L}{\pi} \frac{\ln\left[\sec\left(\frac{\pi\phi^+}{2}\right)\right]}{1 + \frac{L}{\pi b^+} \ln\left[\sec\left(\frac{\pi\phi^+}{2}\right) + \tan\left(\frac{\pi\phi^+}{2}\right)\right]}, \tag{3.4a}$$

$$b^{\perp}_{eff} \simeq \frac{L}{2\pi} \frac{\ln\left[\sec\left(\frac{\pi\phi^+}{2}\right)\right]}{1 + \frac{L}{2\pi b^+} \ln\left[\sec\left(\frac{\pi\phi^+}{2}\right) + \tan\left(\frac{\pi\phi^+}{2}\right)\right]}, \tag{3.4b}$$

which are again in agreement with predictions of (2.27).

https://doi.org/10.1017/jfm.2012.228 Published online by Cambridge University Press

Ng & Wang (2009) addressed the problem of effective slip lengths for stripes with $b^+ \gg L$ and partial b^-, and obtained

$$b^{\parallel}_{eff} \simeq b^{\parallel}_{ideal} + \frac{b^-}{\phi^-}, \quad b^{\perp}_{eff} \simeq b^{\perp}_{ideal} + \frac{b^-}{\phi^-}. \tag{3.5}$$

It can be seen that this result also satisfies (2.27).

For a weak-slip anisotropic texture, $b(x, y) \ll L$, the area-averaged isotropic slip length has been predicted (Belyaev & Vinogradova 2010*a*). This means that the slip-length tensor becomes isotropic and for all in-plane directions, the flow aligns with the applied shear stress. A similar conclusion has been made by Kamrin *et al.* (2010). They proposed asymptotic solutions for $\boldsymbol{b}_{eff}$ for a weak-slip interface, $\varepsilon = \max|b^*(n)| \ll 1$. The two-term expansions of the effective slip lengths in ε can be obtained for an arbitrary local slip:

$$b^{||}_{eff}/L = b^*(0) - \sum_{n=-\infty}^{\infty} |k_n|\,|b^*(n)|^2, \quad b^{\perp}_{eff}/L = b^*(0) - 2\sum_{n=-\infty}^{\infty} |k_n|\,|b^*(n)|^2. \tag{3.6}$$

Since $b^*_2(n) = 2b^*(n)$, (3.6) is also consistent with the relation (2.27).

These examples fully support our predictions, but of course (2.27) is universal and should hold for any one-dimensional surface.

Moreover, (2.27) still holds when the flow is unsteady. Ng & Wang (2011) have considered pressure-driven oscillatory flow in a channel with walls patterned by stripes of $b^+ \gg L$ and $b^- = 0$. For a thick channel they found that both real and imaginary parts of the effective slip lengths roughly satisfy (3.3). The reason is that (2.14), (2.16) and (2.21)–(2.24) remain valid in this case if one replaces $|k_n|$ by $\sqrt{k_n^2 + \mathrm{i}\omega}$.

3.2. *Flow field*

We remark and stress that (2.26) allows one to express the entire flow field for the transverse configuration of patterns in terms of the longitudinal flow field, $u_2(y, z) = u[y, z, 2b(y)]$. Indeed, by applying the inverse Fourier transform of (2.21) and (2.22), one can easily derive by using (2.14), (2.17) and (2.26):

$$v = \frac{1}{2}\left(u_2 + z\frac{\partial u_2}{\partial z}\right), \quad w = -\frac{z}{2}\frac{\partial u_2}{\partial y}, \tag{3.7}$$

$$p = -\frac{\partial u_2}{\partial y}. \tag{3.8}$$

Whence we conclude that at the wall

$$z = 0: \quad v = \frac{1}{2}u_2, \quad \frac{\partial v}{\partial z} = \frac{\partial u_2}{\partial z}. \tag{3.9}$$

Several important conclusions follow from (3.7), (3.8) for alternating perfect-slip ($b^+ \gg L$) and no-slip stripes ($b^- = 0$). In this case $u_2 = u$, and hence, at the wall the velocity along this one-dimensional texture is always twice that perpendicular to it, $u = 2v$. The same relation between velocities in eigendirections has been found by Teo & Khoo (2009) and Ng, Chu & Wang (2010) for the pressure-driven flow in a wide grooved superhydrophobic channel. Analytical solutions have been obtained for the longitudinal velocity u and its gradient $\partial u/\partial y$ at the wall for the shear flow (Sbragaglia & Prosperetti 2007). Equation (3.8) enables us to obtain the pressure for the transverse

https://doi.org/10.1017/jfm.2012.228 Published online by Cambridge University Press

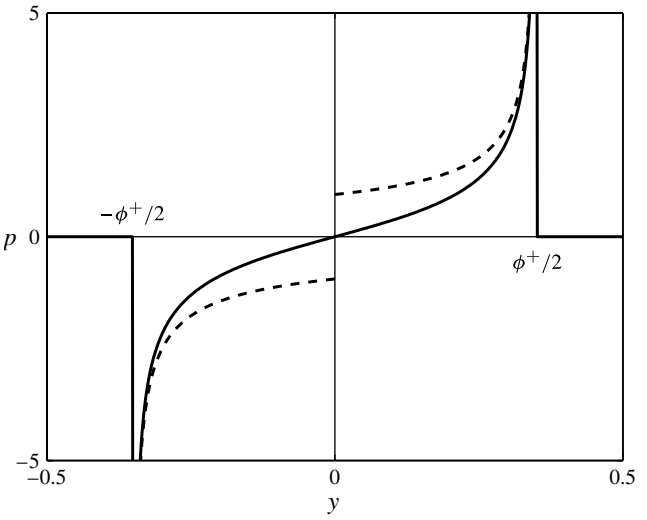


FIGURE 2. Pressure distribution in the transverse flow over alternating perfect-slip, $|y| \leqslant \phi^+/2$, and no-slip, $\phi^+/2 \geqslant |y| \geqslant 1/2$, stripes. Solid and dashed lines are (3.10) and (3.11), respectively.

flow over the perfect-slip region, $|y| \leqslant \phi^+/2$:

$$z = 0: \quad p = -\frac{\partial u}{\partial y} = \frac{\sin(\pi y)}{\sqrt{\cos^2(\pi y) - \cos^2(\pi\phi^+/2)}}. \tag{3.10}$$

The pressure over the no-slip regions, $\phi^+/2 \geqslant |y| \geqslant 1/2$, where $\partial u/\partial y = 0$, is zero. The distribution (3.10) calculated for $\phi^+ = 0.7$ is shown in figure 2. It grows infinitely near the jump in $b(y)$ (from $b^+ \gg L$ to $b^- = 0$) at $y = \pm\phi^+/2$:

$$p \simeq \pm \sin(\pi\phi^+/2)\,[\pi \sin(\pi\phi^+)s]^{-1/2} \quad \text{as } s = (\phi^+/2 - |y|) \to +0. \tag{3.11}$$

Note that a solution for a velocity in an arbitrary direction of the undisturbed flow, $\boldsymbol{U} = z(\boldsymbol{e}_x \cos\theta + \boldsymbol{e}_y \sin\theta)$, represents a superposition of solutions in eigendirections:

$$\boldsymbol{u}_1 = u\boldsymbol{e}_x \cos\theta + (v\boldsymbol{e}_y + w\boldsymbol{e}_z)\sin\theta. \tag{3.12}$$

Therefore, knowledge about the longitudinal velocity at the wall allows us to calculate the flow field in any direction given by an angle θ.

3.3. *Surfaces with an arbitrary one-dimensional texture*

Up to this point, our focus has been on periodic one-dimensional surfaces. Now, we can remove all periodicity requirements that we used to derive (2.26) by applying a Fourier analysis. Indeed, if u_2 is the solution of the longitudinal problem with a non-periodic slip length $2L\beta(y)$, satisfying

$$\Delta u_2 = 0, \tag{3.13}$$

$$z = 0: \quad u_2 - 2\beta(y)\frac{\partial u_2}{\partial z} = 2\beta(y), \tag{3.14}$$

then one can verify directly that transverse solutions, (3.7), (3.8), taking into account (3.9), satisfy the Stokes equation (2.2) and boundary conditions (2.3), (2.4). Thus, our

https://doi.org/10.1017/jfm.2012.228 Published online by Cambridge University Press

results are valid for any arbitrary patterned, not necessarily periodic, one-dimensional surfaces.

Acknowledgement

This research was supported by the Russian Academy of Sciences through its Priority Programme 'Assembly and Investigation of Macromolecular Structures of New Generations'.

REFERENCES

ASMOLOV, E. S. 2008 Shear-induced self-diffusion in a wall-bounded dilute suspension. *Phys. Rev.* E **77**, 66312.

ASMOLOV, E. S., BELYAEV, A. V. & VINOGRADOVA, O. I. 2011 Drag force on a sphere moving towards an anisotropic super-hydrophobic plane. *Phys. Rev.* E **84**, 026330.

BAHGA, S. S., VINOGRADOVA, O. I. & BAZANT, M. Z. 2010 Anisotropic electro-osmotic flow over super-hydrophobic surfaces. *J. Fluid Mech.* **644**, 245–255.

BAZANT, M. Z. & VINOGRADOVA, O. I. 2008 Tensorial hydrodynamic slip. *J. Fluid Mech.* **613**, 125–134.

BELYAEV, A. V. & VINOGRADOVA, O. I. 2010*a* Effective slip in pressure-driven flow past super-hydrophobic stripes. *J. Fluid Mech.* **652**, 489–499.

BELYAEV, A. V. & VINOGRADOVA, O. I. 2010*b* Hydrodynamic interaction with super-hydrophobic surfaces. *Soft Matt.* **6**, 4563–4570.

BELYAEV, A. V. & VINOGRADOVA, O. I. 2011 Electro-osmosis on anisotropic super-hydrophobic surfaces. *Phys. Rev. Lett.* **107**, 098301.

COTTIN-BIZONNE, C., BARENTIN, C. & BOCQUET, L. 2012 Scaling laws for slippage on superhydrophobic fractal surfaces. *Phys. Fluids* **24**, 012001.

COTTIN-BIZONNE, C., BARENTIN, C., CHARLAIX, E., BOCQUET, L. & BARRAT, J. L. 2004 Dynamics of simple liquids at heterogeneous surfaces: molecular-dynamics simulations and hydrodynamic description. *Eur. Phys. J. E* **15**, 427–438.

DAVIS, A. M. J. & LAUGA, E. 2010 Hydrodynamic friction of fakir-like superhydrophobic surfaces. *J. Fluid Mech.* **661**, 402–411.

FEUILLEBOIS, F., BAZANT, M. Z. & VINOGRADOVA, O. I. 2009 Effective slip over superhydrophobic surfaces in thin channels. *Phys. Rev. Lett.* **102**, 026001.

KAMRIN, K., BAZANT, M. Z. & STONE, H. A. 2010 Effective slip boundary conditions for arbitrary periodic surfaces: the surface mobility tensor. *J. Fluid Mech.* **658**, 409–437.

LAUGA, E. & STONE, H. A. 2003 Effective slip in pressure-driven Stokes flow. *J. Fluid Mech.* **489**, 55–77.

NG, C. O., CHU, H. C. W. & WANG, C. Y. 2010 On the effects of liquid–gas interfacial shear on slip flow through a parallel-plate channel with superhydrophobic grooved walls. *Phys. Fluids* **22**, 102002.

NG, C. O. & WANG, C. Y. 2009 Stokes shear flow over a grating: implications for superhydrophobic slip. *Phys. Fluids* **21**, 013602.

NG, C. O. & WANG, C. Y. 2011 Oscillatory flow through a channel with stick-slip walls: complex Navier's slip length. *Trans. ASME: J. Fluids Engng* **133**, 014502.

PHILIP, J. R. 1972 Flows satisfying mixed no-slip and no-shear conditions. *Z. Angew. Math. Phys.* **23**, 353–372.

PRIEZJEV, N. V. 2011 Molecular diffusion and slip boundary conditions at smooth surfaces with periodic and random nanoscale textures. *J. Chem. Phys.* **135**, 204704.

PRIEZJEV, N. V., DARHUBER, A. A. & TROIAN, S. M. 2005 Slip behavior in liquid films on surfaces of patterned wettability. *Phys. Rev.* E **71**, 041608.

SBRAGAGLIA, M. & PROSPERETTI, A. 2007 A note on the effective slip properties for microchannel flows with ultrahydrophobic surfaces. *Phys. Fluids* **19**, 043603.

SCHMIESCHEK, S., BELYAEV, A. V., HARTING, J. & VINOGRADOVA, O. I. 2012 Tensorial slip of super-hydrophobic channels. *Phys. Rev.* E **85**, 016324.

https://doi.org/10.1017/jfm.2012.228 Published online by Cambridge University Press

STONE, H. A., STROOCK, A. D. & AJDARI, A. 2004 Engineering flows in small devices. *Annu. Rev. Fluid Mech.* **36**, 381–411.

TEO, C. & KHOO, B. 2009 Analysis of Stokes flow in microchannels with superhydrophobic surfaces containing a periodic array of micro-grooves. *Microfluid Nanofluid* **7**, 353.

VINOGRADOVA, O. I. & BELYAEV, A. V. 2011 Wetting, roughness and flow boundary conditions. *J. Phys.: Condens. Matt.* **23**, 184104.

https://doi.org/10.1017/jfm.2012.228 Published online by Cambridge University Press